



FR9601304



CRN 95-14

Factors Influencing the Performances of
Micro-Strips Gas Chambers

and

Microstrips Gaz Chambers on Implanted
Substrates

J.M. Brom, R. Fang, J.C. Fontaine, W. Geist, D. Huss,
T. Kachelhoffer, H. Kettunen, J.M. Levy, V. Mack, A. Pallarès

Technical staff :

A.M Bergdolt, J. Cailleret, E. Christophel, J. Coffin, H. Eberlé, F. Osswald,
M.H. Sigward

*Centre de Recherches Nucléaires de Strasbourg
Université Louis Pasteur
Université de Haute Alsace*

S. Barthe, J.P. Schunck

Laboratoire PHASE (UPR 292 du CNRS) Strasbourg

Presented at the Vienna Wire Chamber Conference '95

**CENTRE DE RECHERCHES NUCLEAIRES
STRASBOURG**

IN2P3

CNRS 

UNIVERSITE

LOUIS PASTEUR

Gestion INIS
Doc. enreg. le : 9/8/95
N° TRN : PR9...4...6..
Destination : I,I+D,D

Factors Influencing the Performances of Micro-Strips Gas Chambers

March 1995

V. Mack, J.M. Brom, R. Fang, J.C. Fontaine, D. Huss T. Kachelhoffer,
H. Kettunen, J.M. Levy, A. Pallarès

Technical staff :

A.M Bergdolt, J. Cailleret, E. Christophel, J. Coffin, H. Eberlé, F. Osswald,
M.H. Sigward

*Centre de Recherches Nucléaires de Strasbourg
Université Louis Pasteur
Université de Haute Alsace*

S. Barthe, J.P. Schunck

Laboratoire PHASE (UPR 292 du CNRS) Strasbourg

Abstract

Damages to MSGCs induced by discharges have been investigated. Optimization of electrode shapes and/or deposition of a protective coating allows to increase the potential difference between anode and cathode, thus increasing the gain.

For prototypes of MSGCs made at the Centre de Recherches Nucléaires, each step of the manufacturing processes was carefully controlled. Results are presented on the influence of cleaning processes on the surface resistance of glass substrates.

Presented at the Vienna Wire Chamber Conference '95

1 Introduction

The microstrips gas chambers (MSGC) introduced by Oed [1] operate like conventional multiwire proportionnal chambers (MWPC). Electrode strips etched by photolithography on a substrate replace wires, and pitch between anode and cathode is an order of magnitude smaller for MWPCs. The drift region is shaped by a cathode plane placed at a few millimeters from the substrate. Primary electrons are multiplied in the amplification region close to anode strips.

The gain of gaseous counters is a function of at least three parameters : detector geometry, gas mixture and voltages.

For MWPCs the gain depends on the wire radius. In a similar way, the gain of MSGCs depends on anode and cathode widths. Several studies [2, 3] show that one can increase the gain by reducing the width of anodes to 10 or $5\mu\text{m}$, and by increasing the width of cathodes to 100 or $150\mu\text{m}$.

The gain dependance on cathode voltage for various mixtures of argon and dimethylether (DME) was studied. The maximum gain before breakdown is typically in the order of $3 \cdot 10^3$ to $5 \cdot 10^3$.

2 Breakdowns of MSGCs

There are essentially two sources of damage in wire chambers. The first is formation, in electronic avalanches, of polymeric compounds that produce a deposit on wires. This may effect a loss of gain, depending on the gas mixture [4]. This problem exists also for MSGCs [5]. To prevent it a "clean" gas mixing system has to be used, and all possible polluting agents have to be eliminated. DME-based mixtures are favored over hydrocarbons [6].

A second source of damage is breakdown between electrodes. In MSGCs, a spark between anode and cathode may lead to an evaporation of metal, this eroding and cutting one or more of the strips [7].

To increase the maximum stable gain before discharge, two solutions, maybe complementary, are presented : optimization of electrode design and protection of points where sparks occur.

Three lay-outs of electrodes have been studied sofar (see fig.1). An electrostatic simulation programme ("COSMOS") was used to calculate the field at the ends of cathodes and anodes for the following conditions. Cathode width: $70\mu\text{m}$, anode width: $9\mu\text{m}$, pitch: $200\mu\text{m}$, drift voltage: -1200 V on a 3 mm gap, cathode voltage: -420 V , anode voltage: 0 V and glass substrate was assumed for the simulation. The points of maximum field strengths are indicated in fig.1 by arrows. The electrostatic simulation was made in two dimensions. The thickness strip effect was neglected and maximum field values are underestimated. However this calculation allows comparisons.

To localise discharges visually, a MSGC with semitransparent window was used. Measurements are performed with an Ar-DME (90-10) mixture and a drift voltage of -1200 V . Cathode strip voltages were increased until sparking

was observed. It was found that sparking starts first at the end of cathodes (fig.2) whereas electrostatic simulation predicts sparking to begin at the ends of anodes. Discharge at the end of cathodes occurs, on the other hand, at the field values predicted by electrostatic simulations. One is lead to conclude that electrostatic simulations are not sufficient to correctly predict MSGC performance. It may therefore be necessary to consider electrodynamic processes [8].

The measurements show (tab.1) that designs n° 1 and 2 (longer cathodes) support high voltages before breakdown. An increase cathode voltages of 30 V improves the gas gain by up to a factor 2. The region where sparks were detected was then covered by a dielectric glue (Epotecny 505) and the procedure was iterated. For the three designs, protection of the end of cathodes allows to increase cathode voltages to 490 V. And then sparking starts at defective points along the strips. For design n°0, this points were covered by glue and the procedure was iterated (tab.2). Protection allows to increase cathode voltages by up to 80 V, compared to the initial value 450 V, corresponding to an increase of gain by a factor 4.5.

Breakdown is a particulrly serious problem on the cathode ends side. To prevent discharges, we found that electrode design n° 1 is better and passivation of critical regions, with protective coating is more effective.

3 Influence of cleaning processes on surface resistance of glass

Before etching four different cleaning solutions have been tested. These included chemicals which are ordinarily used during the different phases of lithography. Ultrasonic bath was also always applied in the cleaning process.

The mildest chemicals used for cleaning are distilled water and solvents like alcohols and acetone. These do not have any effects on glasses. One solution was Merck's Extran^R which is a commercial cleaning agent for glasses and optical instruments. It contains alkalines like sodium hydroxide. Another cleaning liquid is pure sulphochrome (sulphuric acid + potassium dichromate) or sulphochrome plus hydrofluoric acid. The adhesion of strips is usually better with stronger chemicals as they attack the surface of glasses and remove inorganic impurities.

The surface resistance of the two glasses, Schott D263 and Corning 7059, was measured as function of cleaning treatment. A current was measured between two probes 5 mm apart from each other for a voltage of 200 V. The resistances obtained are shown in table 3, they vary by up to three orders of magnitude.

Water plus solvent cleaning gave the nominal surface resistances of Schott D263 and Corning 7059 glasses which were $2.8 \cdot 10^{14}$ and $10^{15} \Omega$ respectively, according to the manufacturer. On the contrary, additional cleaning agents had clear effects on the resistances of the substrates.

The change caused by Merck's Extran^R is understood as due to diffusion of

sodium ions into the Schott D263 glass. Sodium ions can not diffuse into the Corning 7059 glass according to the manufacturer, and so no modification of resistance has been observed. Clearly, diffusion of sodium ions into the Schott D263 glass is enhanced when heating the substrate.

The modification due to sulphochrome were probably caused by ion diffusion into glass. It is known that chromium ions diffuse in silicate substrates, as observed for silicon [9]. Diffusion of such multivalent ions reduce the surface resistivity of the substrate.

Hydrofluoric acid used after sulphochrome, etches glass and then removes part of the previously diffused chromium ions. This leads to the observed increase of the surface resistivity; it is more important for the Corning 7059 glass than for the Schott D263 glass. According to the manufacturer, Corning 7059 glass has to be cleaned without any acid solution that may damage the surface.

4 Conclusion

Some factors influencing counter performances are comparable for MWPC and MSGC : such as of polymerization in gas, and detector geometry. On the other hand, the problem of breakdown is more important for MSGCs. Optimization of electrode shapes and deposition of protective coating allows to increase the maximum field for stable gain.

For MSGC, surface resistance seems to be the most essential problem. It has been shown previously that surface resistance evolution leads to dramatic changes of gain, especially under irradiation.

It has been shown here that surface resistance can vary up to 3 orders of magnitude due to the chemicals used in the cleaning process before metalisation. Studies are now under way at CRN-Strasbourg to understand effects of the etching process. One concludes from these investigations that all operations related to the fabrication of MSGCs have to be carefully controlled in order to ensure a viable solution for a MSGC-based tracking device for LHC experiments.

References

- [1] A. Oed, Nucl. Instr. and Meth. A263, (1988), 351
- [2] T. Beckers, R. Bouclier, Ch. Garabatos, G. Million, F. Sauli and L.I. Shekhtman, Nucl. Instr. and Meth. A346, (1994), 95
- [3] J.J. Florent, J. Gaudaen, L. Ropelewski and F. Sauli, Nucl. Instr. and Meth. A329, (1993), 125
- [4] J.A. Kadyk, Nucl. Instr. and Meth. A300, (1991), 436
- [5] R. Bouclier, C. Garabatos, G. Manzin, G. Million, F. Sauli, T. Temmel and L. Shekhtman, Nucl. Instr. and Meth. A348, (1994), 109
- [6] R. Bouclier, M. Capeáns, C. Garabatos, R.D. Heuer, M. Jeanrenaud, T.C. Meyer, F. Sauli and K. Silander, Nucl. Instr. and Meth. A346, (1994), 114
- [7] S. Snow, I. Duerdoth, N. Lumb and R. Thompson, Nucl. Instr. and Meth. A348, (1994), 356
- [8] R. Fang, R. Blaes, J.M. Brom, W. Geist, A. Michalon, J.L. Riestler and C. Voltolini CRN 93-061, (1993)
- [9] F.L. Freire Jr., Nucl. Instr. and Meth. B83, (1993), 361

Design n°	0	1	2
Cathode voltages first sparks	-455 ±5 V	-485 ±5 V	-475 ±5 V
Gas Gain	1700	3300	2700

Tab.1 : Limit of cathode voltages before sparks and corresponding gain.

	Cathode Voltages First Spark	Localisation of Discharges
no protection	-450 ±5 V	end of cathodes
protection of : ends of cathodes	-480 ±5 V	defective points along the strips
protection of : ends of cathodes + defective points along strips	-530 ±10 V	ends of anodes
protection of : ends of cathodes + defective points + ends of anodes	-530 ±10 V	

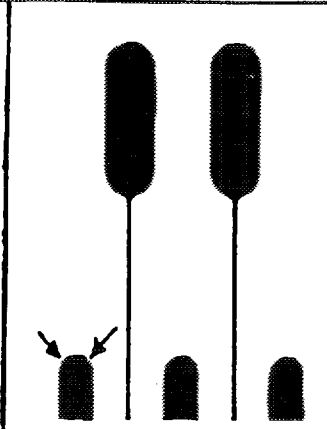
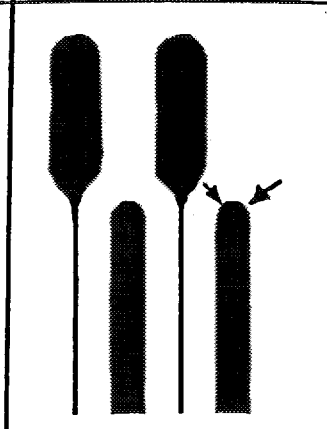
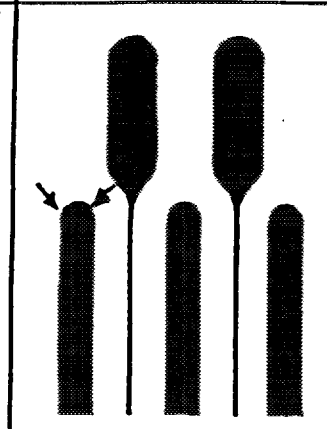
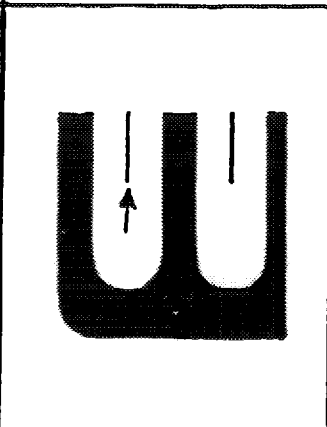
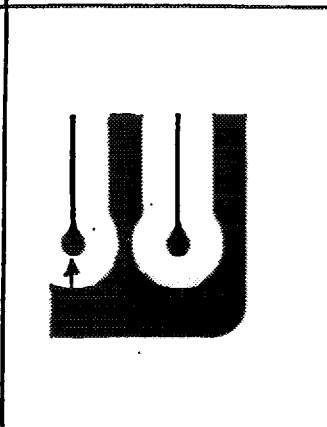
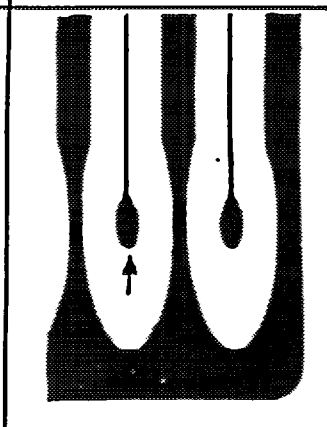
Tab.2 : Localisation of breakdowns in MSGC (design n°0) and effect of coating in the region where discharges occur.

Cleaning	Schott D263	Corning 7059
water and solvent	2.8 10 ¹⁴	10 ¹⁵
Merck's Extran ^R	3.7 10 ¹²	10 ¹⁵
Merck's Extran ^R Baked at 400°C N ₂	1.2 10 ¹²	-
Sulphochrome*	2.6 10 ¹³	9 10 ¹¹
Sulphochrome* + hydrofluoric acid (10%)	2.9 10 ¹³	3.1 10 ¹³

Tab.3 : Surface resistance R in ohm of D263 and 7059 glasses for different cleaning solutions.

Merck's Extran^R : alkaline mixture

*mixture of potassium bichromate (K₂Cr₂O₇) and sulphuric acid (H₂SO₄)

Design n°	0	1	2
Maximum field	105 kV/cm	110 kV/cm	110 kV/cm
Ends of cathodes			
Ends of anodes			
Maximum field	250 kV/cm	130 kV/cm	123 kV/cm

→ : localisation of maximum field

Figure 1: Designs of electrodes, localisation and values of maximum field (COSMOS simulation) at the ends of cathodes and anodes.

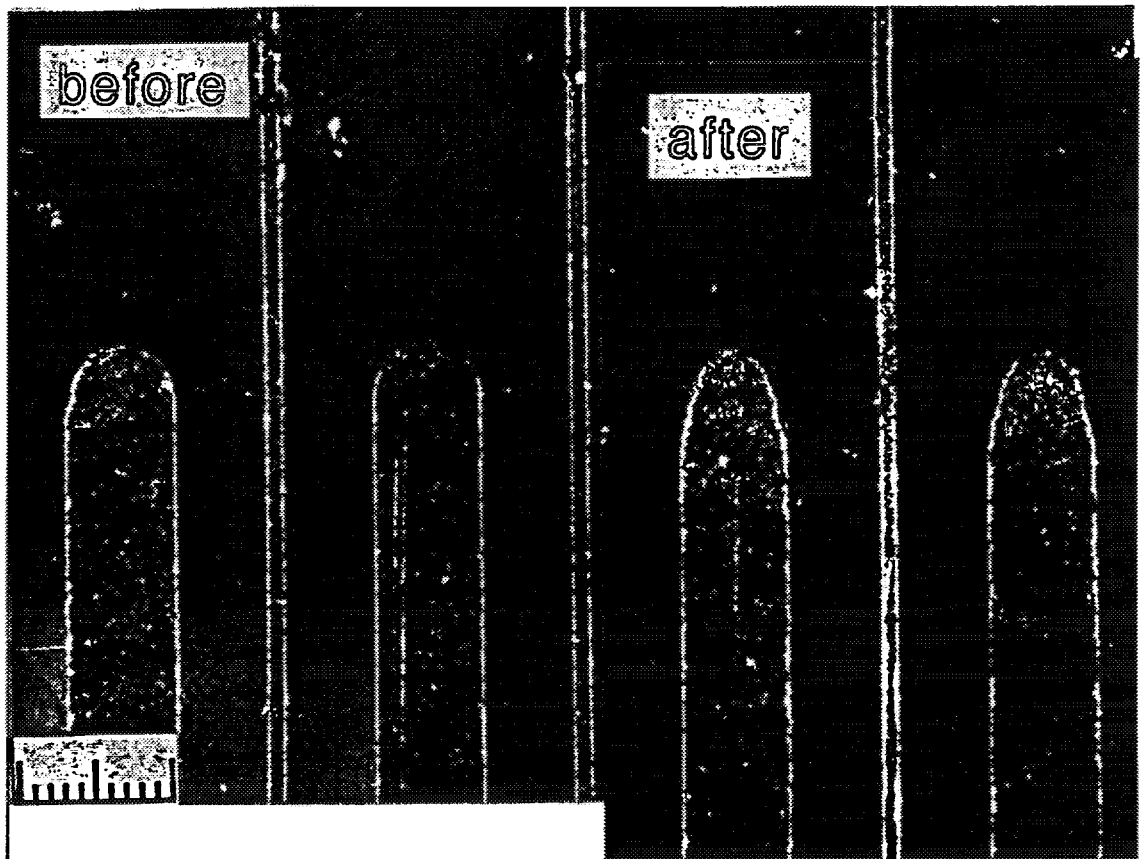


Figure 2: Ends of cathodes before and after discharge (scale = 100 μm).

MICROSTRIP GAS CHAMBERS ON IMPLANTED SUBSTRATES

A. Pallarès, J.M. Brom, R. Fang, J.C. Fontaine, W. Geist, T. Kachelhoffer, J.M. Levy, V. Mack.

Technical staff : S. Barthe*, A.M. Bergdolt, J. Cailleret, E. Christophel, J. Coffin, H. Eberlé, J.P. Schunck*, M.H. Sigward.

Centre de Recherches Nucléaires - Université Louis Pasteur - Université de Haute Alsace, 23, rue du Loess, BP 28, 67037 Strasbourg Cedex 2.

**Laboratoire PHASE (UPR 292 du CNRS), 23, rue du Loess, BP 28, 67037 Strasbourg Cedex 2.*

Abstract

We have studied the performance of several Microstrip Gas Chambers (MSGC) prototypes made on standard Desag D263 boron implanted glass. The purpose of the implantation is to reduce the surface resistance. The long term stability of this implantation has been measured under applied bias voltage. Comparative tests have been carried out on prototypes made on implanted and non-implanted detectors under electron (^{90}Sr) and X-ray (8 keV) irradiation. The total dose was approximately 7 mC/cm .

1. INTRODUCTION

Microstrip Gas Chambers (MSGC) are a recent detector development in particle physics. They derive directly from the multiwire proportional chamber (MWPC) concept initiated by G. Charpak [1,2]. In a MWPC a plane of anode wires lies between two cathode planes. Each anode wire acts as an individual proportional counter, thereby allowing spatial resolution, of the order of half the wire spacing, of about 1 mm. The cathode drift planes define the drift region for primary electrons. High voltage applied to the cathode wires defines an electrical field that induces the electron avalanche and leads to an observable signal on the anode wires via the avalanche formation.

However, the spatial resolution of MWPC is limited for mechanical reasons. MSGC improve this resolution by reducing pitch and wire dimensions. These detectors are made from thin metallic strips (alternately anodes and cathodes) engraved on a dielectric substrate by means of standard microelectronic techniques. A cathode plane at a few millimeters above the substrate defines the electric drift field.

The dielectric support of the MSGC (glass, plastic, etc.) was supposed to have mainly a mechanical role with negligible influence on the detector performance. But in the early years of MSGC, experience showed gain instabilities and variations probably due to charge accumulation at the surface of the substrate. These effects modify locally the electric field. For glasses with electronic conductivity, the gain reduction is small or inexistent [3,4]. Hence the substrate resistivity is of primary importance.

Several methods were used to control the substrate's electrical resistance : manufacture of special low resistance glass (the so-called Moscow glass developed by the BIP-Novosibirsk), application of passivation layers [5,6] and ion implantation [7,8]. The latter method, namely boron implantation of standard high resistivity Schott D263 glass is chosen here.

2. EXPERIMENTAL PROCEDURES

All detectors used for the following measurements were fully homemade. They have been manufactured by the PHASE laboratory in collaboration with the Centre de Recherches Nucléaires of the CNRS Strasbourg. This facilitates knowledge and control of all parameters during the detector fabrication (cleaning, metallization, etching, etc.). Figure 1 shows such a typical laboratory-made MSGC.

2.1. ION IMPLANTATION

Ion implantation is a well-known process that modifies surface properties. It is a precise and reproducible method in which one has an easy control of the implantation energy, dose and density profile of the implanted element.

Standard D263 glasses were implanted (before or after detector fabrication) with boron at an energy of 18 keV and at a dose of 10^{15} ions/cm². Under these conditions, the boron is typically concentrated in a glass surface layer about 1000 Å thick.

2.2. MEASUREMENTS OF SURFACE RESISTANCE

All measurements of surface resistance were made on bare glass plates using a three electrode arrangement (standard insulator resistance measurement method ASTM D257) shown schematically in figure 2. A known potential (200 V in the present case) is applied to the sample and the resulting current is measured with a picoammeter. The guarding of electrode 3 plays an important role : it minimizes errors due to bulk resistance while making surface resistance measurements.

When a potential difference is applied to the sample, the resulting current decreases asymptotically towards a limiting value. This decrease of current with time is due to dielectric absorption (interfacial polarization, volume charge, etc.) and the sweep of mobile ions to the electrodes. Thus it is necessary to specify the time of electrification, which is about 1000 min in our standard measurements. This amount of time is required to reach a stable dielectric state.

The measured surface resistance is largely dependent on the contamination that happens to be on the glass surface. However the permittivity of the glass influences deposition of contaminants and its surface characteristics affect the conductance of the contaminants. Surface resistance also depends on the working atmosphere (humidity, temperature and gas). In summary, surface resistance measurements are more qualitative than quantitative. Absolute values may not be accurate but relative ones remain comparable. Measurements are only comparable when the procedure used is identical (applied voltage, electrification time, atmosphere, etc.).

2.2.1. Effects of ion implantation

For Schott D263 glass, surface resistance exceeded $5 \cdot 10^{15}$ Ω before implantation and was about $2 \cdot 10^{14}$ Ω after at a boron dose of 10^{15} ions/cm². It is obvious that one is able to control glass surface resistance by implantation dose. As an example, figure 3 shows a typical decrease of glass surface resistance with increasing ion implantation dose for iron ions (at an energy of 150 keV on Corning 7059 glass).

2.2.2. Resistance stability

Doping by ion implantation consists of introducing ions in a stable glass matrix. However the implanted elements may continue to migrate under external forces like electrical fields. This migration can lead to important modifications of the surface resistance with time. We have checked the stability of the surface resistance under bias voltage over a period of days. The glass polarization was always kept at 200 V. Figure 4 shows that after a short stabilization period, the surface resistance remains constant with time (within the accuracy limits).

3. EFFECT OF ION IMPLANTATION ON DETECTOR PERFORMANCE

We observed a significant improvement of the performance of implanted detectors compared to non-implanted ones.

The gain evolution of implanted and non-implanted detectors as a function of ^{90}Sr (e^- , $E_{\text{max}}=2.282$ MeV; 10 mCi) irradiation dose is shown in figure 5. In both cases, a gain reduction under irradiation is observed. However, the gain drop of the implanted detector is clearly smaller compared to the non-implanted one (10% after 0.1 mC/cm for the implanted one compared to 60% for the non-implanted one).

Figure 6 shows the gain stability of an implanted detector irradiated with 8 keV X-ray at a rate of 10^6 mm $^{-2}$ ·s $^{-1}$. After a small decrease (about 5%) at the beginning of the irradiation, the gain remains stable. The difference compared to ^{90}Sr irradiation is supposed to be due to the gas system which is different for each type of irradiation and less clean in ^{90}Sr irradiation case. It has also been shown that the loss of gain may be strongly dependent on the irradiation rate [9].

4. CONCLUSIONS

Ion implantation was shown to improve the gain stability of MSGC made on standard high resistivity glass exposed to high radiation rates.

To obtain surface resistance reduction, previous work shows that the choice of the implanted element, if stable in the glass matrix, may be without importance [10]. The fundamental mechanisms by which ion implantation decreases surface resistance are still not fully understood. Ion implantation causes alkali depletion near the glass surface such that ionic conduction may be avoided [11]. It also creates paramagnetic defects (which may be charged) in the glass structure [12]. Combination of these two effects may provide an adequate conduction mechanism.

REFERENCES

- [1] G. Charpak, *Ann. Rev. Nucl. Sci.* 20 (1970) 195.
- [2] G. Charpak, D. Rahm, H. Steiner, *Nucl. Instr. and Meth.* 80 (1970) 13.
- [3] G. Minakov, Y. Pestov, V. Prokopenko, L. Shekhtman, *Nucl. Instr. and Meth.* A326 (1993) 566.
- [4] R. Bouclier, G. Million, L. Ropelewski, F. Sauli, Y. Pestov, L. Shekhtman, *Nucl. Instr. and Meth.* A332 (1993) 100.
- [5] S. Brons, W. Bruckner, M. Heidrich, I. Konorov, S. Paul, *Nucl. Instr. and Meth.* A342 (1994) 411.
- [6] S. Salomon, J. Armitage, G. Chapman, M. Dixit, J. Dubeau, W. Faszer, L. Hamel, G. Oakham, *Nucl. Instr. and Meth.* A348 (1994) 313.
- [7] J. Van Der Marel, A. Van Den Bogaard, C. Van Eijk, R. Hollander, W. Okx, P. Sarro, *Nucl. Instr. and Meth.* A348 (1994) 383.
- [8] M. Dixit, F. Oakham, J. Armitage, J. Dubeau, D. Karlen, G. Stuart, S. Taylor, I. Shipsey, E. Johnson, A. Greenwald, *Nucl. Instr. and Meth.* A348 (1994) 365.
- [9] F. Sauli, this conference.
- [10] A. Pallarès, S. Barthe, A.M. Bergdolt R. Blaes, J.M. Brom, J. Cailleret, E. Christophel, J. Coffin, H. Eberlé, R. Fang, J.C. Fontaine, W. Geist, T. Kachelhoffer, H. Kettunen, V. Mack, A. Michalon, J.L. Riester, A. Romero, J.P. Schunck, M.H. Sigward, R. Stuck, C. Voltolini, CRN report 93-64 (1993).
- [11] O. Puglisi, G. Marletta, A. Torrisi, *J. Non-Cryst. Solids* 83 (1986) 344.
- [12] G.W. Arnold, *J. Non-Cryst. Solids* 179 (1994) 288.

FIGURE CAPTIONS

- Figure 1 : Laboratory-made MSGC (glass surface $2.6 \cdot 2.6 \text{ cm}^2$, $200 \mu\text{m}$ pitch, anode and cathode respectively $9 \mu\text{m}$ and $70 \mu\text{m}$ width) .
- Figure 2 : The three electrode arrangement for insulator resistance measurements.
- Figure 3 : Typical evolution of surface resistance as a function of implanted dose (the solid line is only to guide the eye).
- Figure 4 : Evolution of the surface resistance as a function of time (bias voltage : 200 V , the solid line is only to guide the eye).
- Figure 5 : Variation of gain as a function of electron irradiation dose (^{90}Sr , 10 mCi).
- Figure 6 : Variation of gain as a function of X-ray irradiation dose (8 keV , $10^6 \text{ mm}^{-2} \cdot \text{s}^{-1}$).

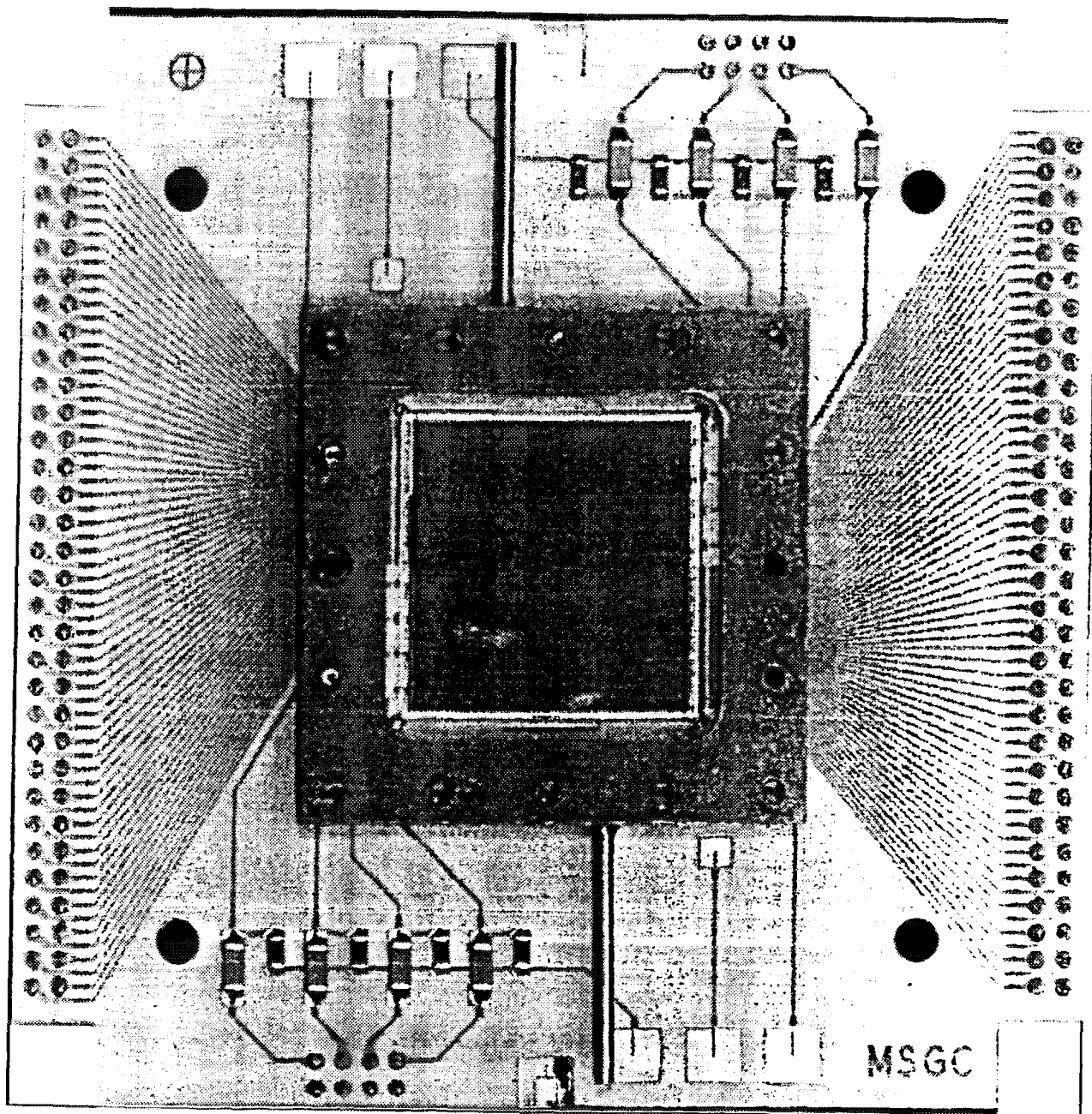


Figure 1

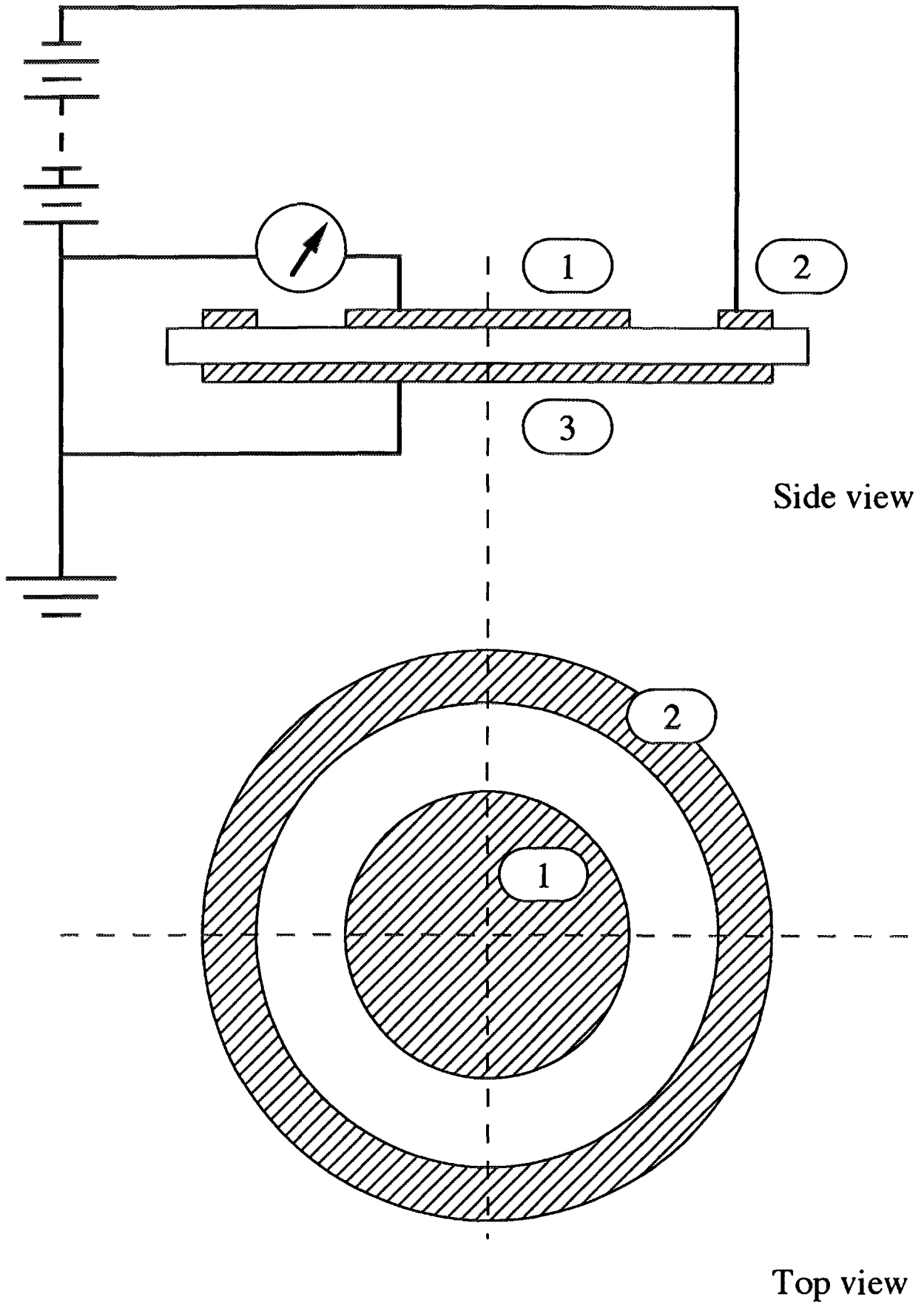


Figure 2

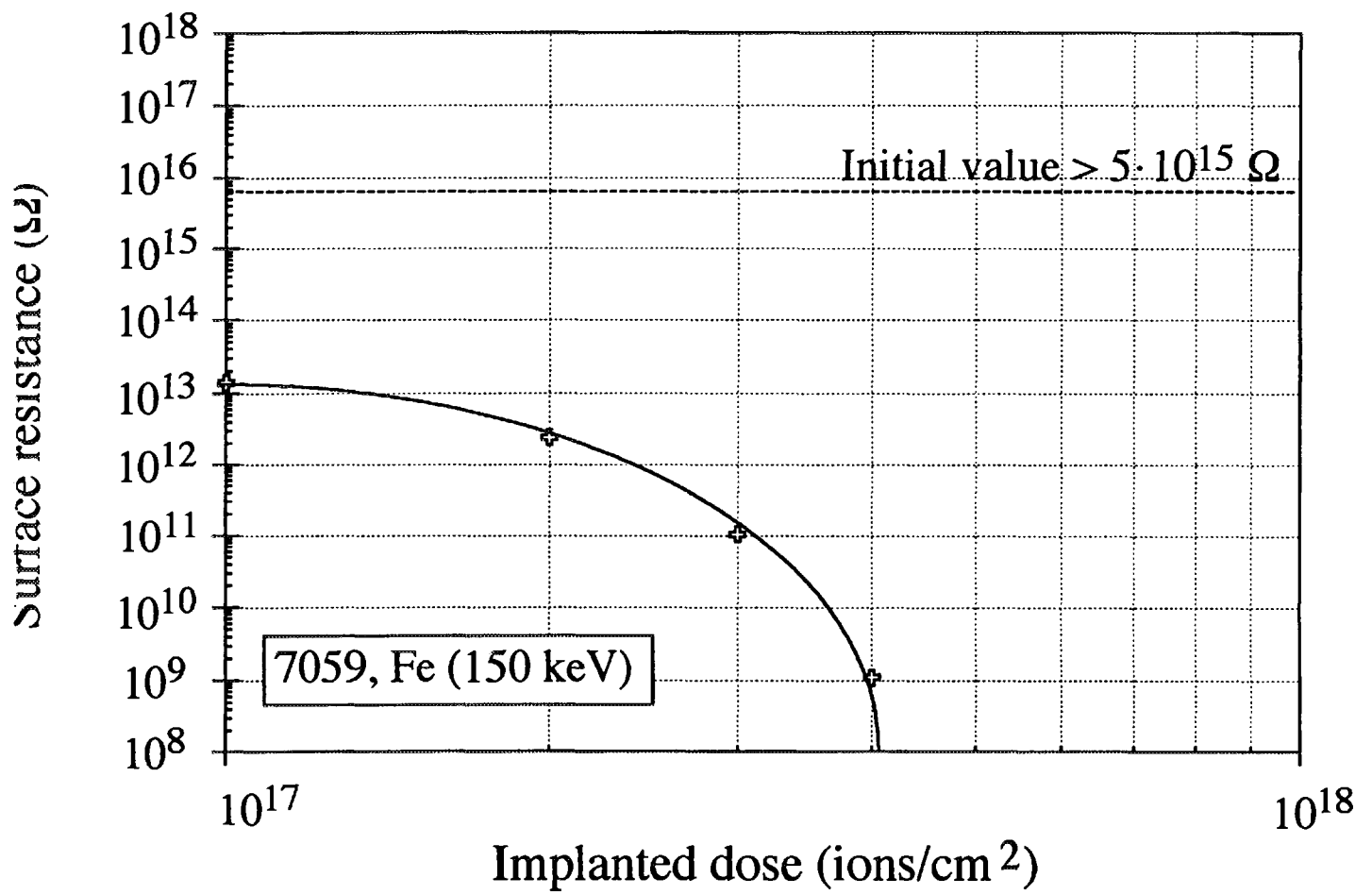


Figure 3

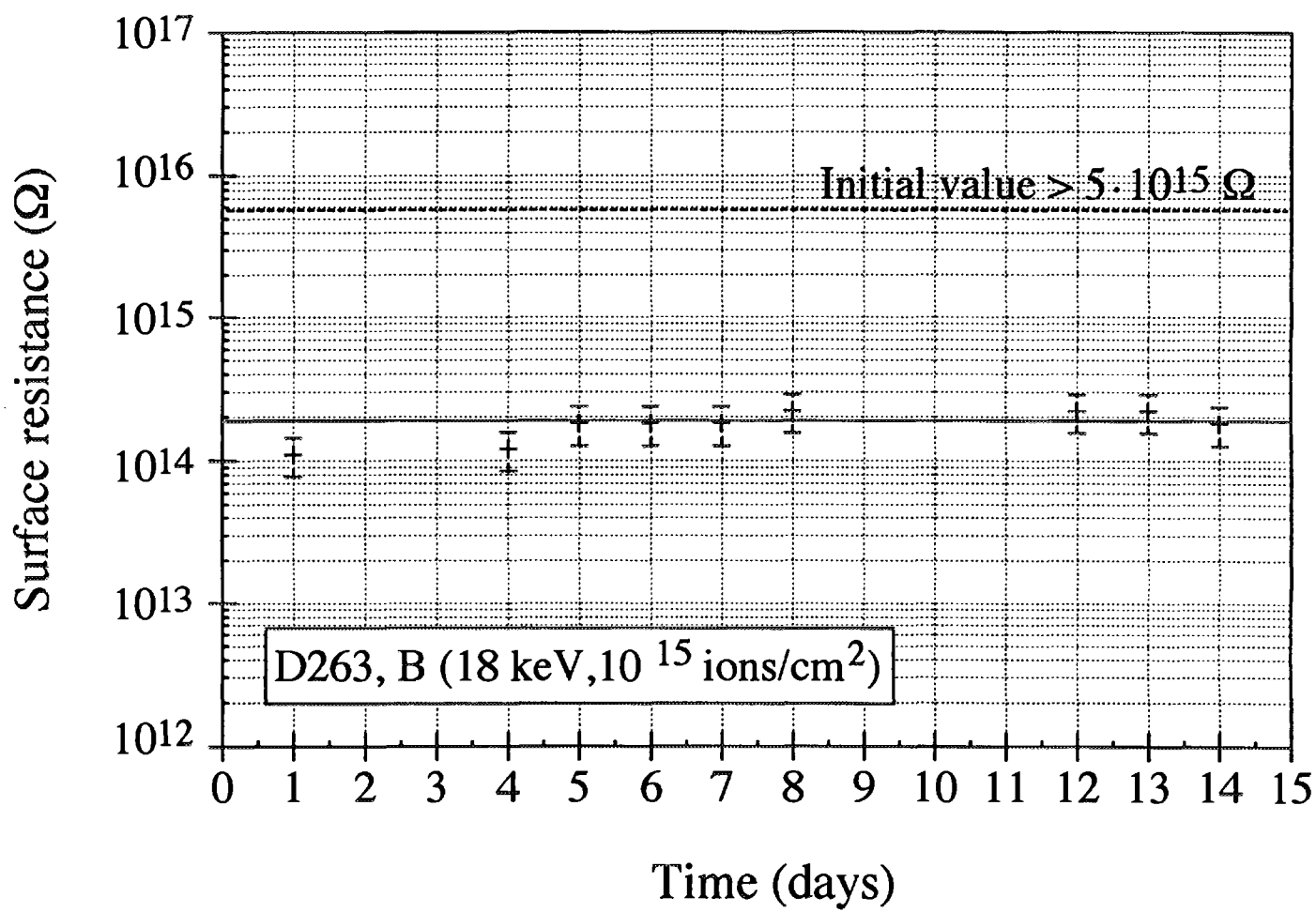


Figure 4

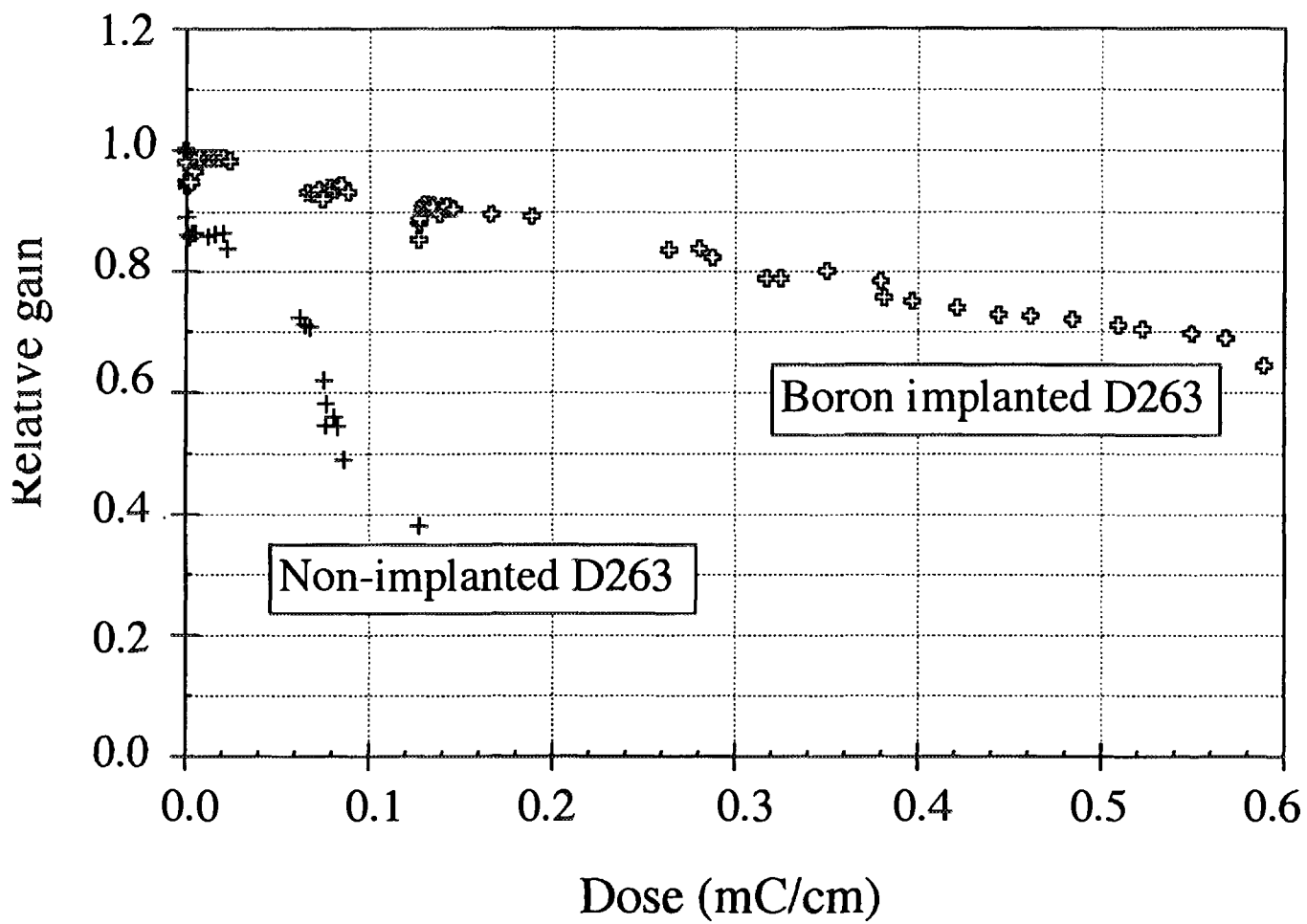


Figure 5

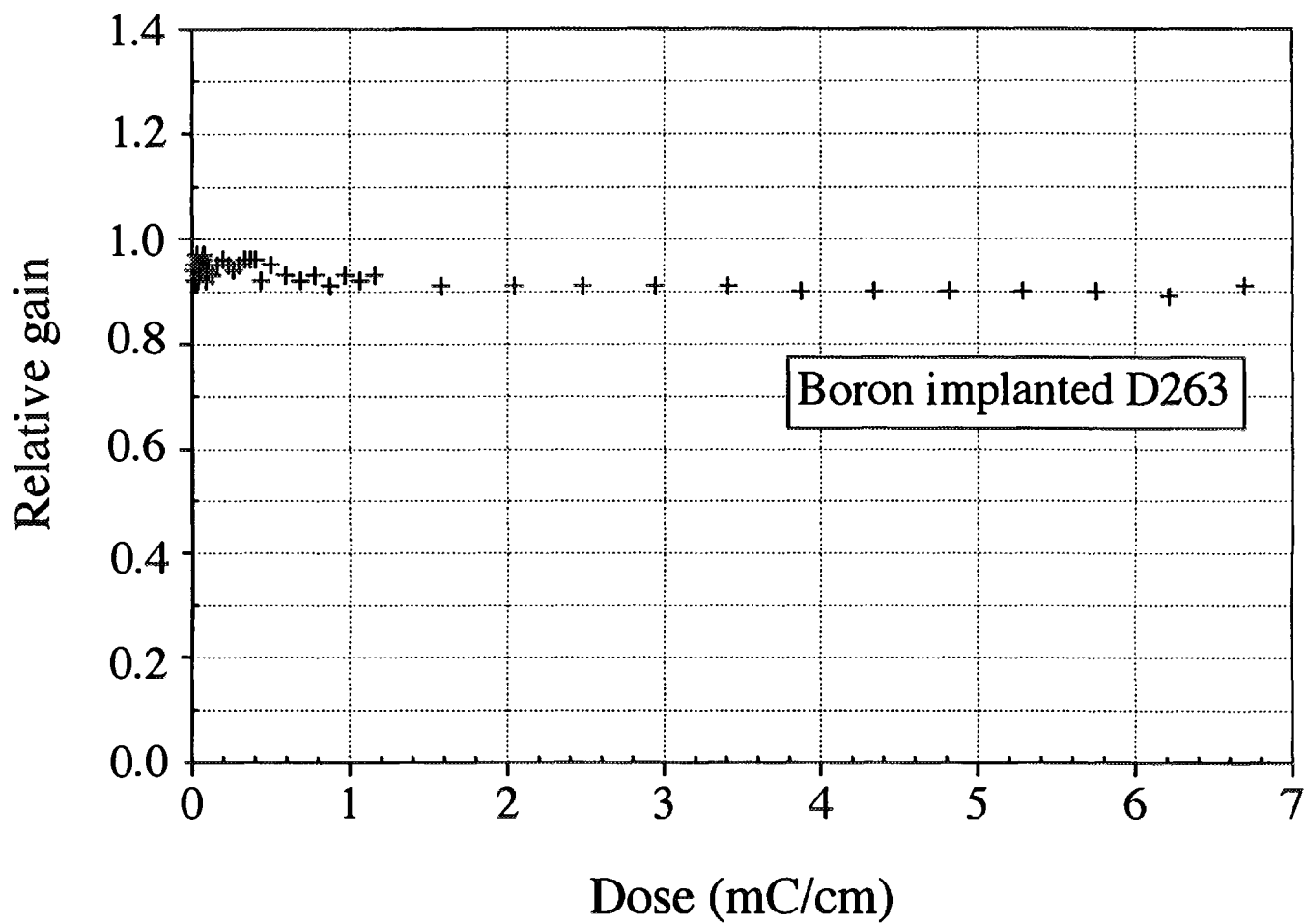


Figure 6